Available online at www.sciencedirect.com
ScienceDirect
Trans. Nonferrous Met. Soc. China 24(2014) 2307−2313
Transactions of Nonferrous Metals Society of China
www.tnmsc.cn

Effects of silicon content on microstructure and stress corrosion cracking resistance of 7050 aluminum alloy

Huan SHE[1], Wei CHU[1], Da SHU[1], Jun WANG[1,2], Bao-de SUN[1,2]

1. Shanghai Key Lab of Advanced High-temperature Materials and Precision Forming, Shanghai Jiao Tong University, Shanghai 200240, China;
2. State Key Laboratory of Metal Matrix Composites, Shanghai Jiao Tong University, Shanghai 200240, China

Received 17 October 2013; accepted 23 April 2014

Abstract: Evolution of microstructure and stress corrosion cracking (SCC) susceptibility of 7050 aluminum alloy with 0.094%, 0.134% and 0.261% Si (mass fraction) in T7651 condition have been investigated. The results show that the area fraction of Mg_2Si increases from 0.16% to 1.48% and the size becomes coarser, while the area fraction of the other coarse phases including Al_2CuMg, $Mg(Al,Cu,Zn)_2$ and Al_7Cu_2Fe decreases from 2.42% to 0.78% with Si content increasing from 0.094% to 0.261%. The tensile strength and elongation of 7050-T7651 alloys is decreased with the increase of Si content by slow strain rate test (SSRT) in ambient air. However, electrical conductivity is improved and SCC susceptibility is reduced with the increase of Si content by SSRT in corrosion environment with 3.5% NaCl solution.

Key words: 7050 aluminum alloy; silicon content; microstructure; stress corrosion cracking resistance

1 Introduction

7××× series aluminum alloys (Al−Zn−Mg−Cu) are widely used in aerospace industry because of their high specific strength. To face the challenge of mass air transportation, the improved damage tolerant properties are needed such as fatigue performance, fracture toughness and stress corrosion cracking (SCC) resistance [1−3]. SCC attracts the attentions of researchers because it limits the application of 7xxx series aluminum alloys significantly.

Many studies focus on the effects of grain-boundary precipitates (GBPs) on SCC of 7xxx series aluminum alloys. SCC resistance can be effectively improved by increasing the size and spacing of the GBPs to decrease the initiation and propagation of intergranular crack [4−7]. Moreover, increasing the Cu content of GBPs also improves SCC resistance by reducing the electrochemical activity to increase the crack initiation resistance, inversely for Zn [8]. Over-aging and retrogression and reaging (RRA) treatments have positive impact on SCC resistance compared with T6 treatment by coarsening and separating GBPs [9−11]. PENG et al [12] reported that SCC resistance of 7B50 aluminum alloy was improved with increasing the time of repetitious-RRA treatment because the GBPs became more discrete and coarser and the Cu content of GBPs increased. HUANG et al [13] improved the SCC resistance of 7055 aluminum alloy by high-temperature pre-precipitation treatment to enhance the discontinuous distribution of the coarse precipitates along the grain boundary and increase the Cu content of GBPs.

In addition, Fe and Si have an unnegligible impact on the SCC resistance as the main impurities in 7xxx series aluminum alloys. The effects of Fe and Si impurities on the stress corrosion cracking resistance are relative to the pitting of Fe-rich and Si-rich phases. The coarse Fe-rich and Si-rich phases are identified to have different Volta potentials with the surrounding α(Al) matrix [14,15]. They are the initiation sites for localized corrosion due to anodic dissolution in corrosion environment, providing the initial crack and promoting the production of hydrogen on the cathode [8,16,17].

However, comprehensive studies on the quantitative effect of impurity contents on the SCC resistance of 7xxx

Foundation item: Project (2012CB619505) supported by the National Basic Research Program of China; Project (NCET-13-0370) supported by the Program for New Century Excellent Talents in Universities of China
Corresponding author: Da SHU; Tel: +86-21-54742683; E-mail: dshu@sjtu.edu.cn
DOI: 10.1016/S1003-6326(14)63349-5

series aluminum alloys and the correlation with the evolution of impurity phases in microstructure are scarce. The aim of this work is to study the effect of impurity Si on the microstructure and stress corrosion cracking resistance of 7050 aluminum alloy as one of the important aircraft structural materials.

2 Experimental

The raw material of 7050 ingot with a composition of 5.615% Zn, 1.912% Mg, 2.068% Cu, 0.09% Zr, 0.106% Fe, 0.065% Si and balanced Al (mass fraction) was remelted in an electrical resistance furnace at the melting temperature of 780 °C. After completely melted, the pure Si particles wrapped by aluminum foil were added into the melt to prepare 7050 alloys containing different Si contents. The alloys were cast into an iron mould with an internal dimension of *d*102 mm × 150 mm. The actual contents of Si in three remelted 7050 alloys (designated as Alloys 1, 2 and 3) were analyzed by spectrophotometry, which were 0.094%, 0.134% and 0.261%, respectively.

The as-cast ingots were homogenized at 430 °C for 24 h and then hot-extruded into plates of 12.7 mm × 25.4 mm at 380−410 °C, with an extrusion ratio of 24.3:1. T7651 temper was carried out for all the extruded plates, which consisted of solution treatment at 473 °C for 3 h, followed by cold water quenching and 2% pre-stretching, then dual aging at 121 °C for 6 h and 174 °C for 15 h [18].

Electrical conductivity was determined using FD-102 eddy current conductivity tester. The slow strain rate test (SSRT) was carried out in the longitudinal direction of extruded plates according to GB/T 15970.7−2000. The dimensions of SSRT specimens are shown in Fig. 1. The SSRT was conducted in air and in an aerated 3.5% NaCl solution, respectively, for each 7050 aluminum alloy with strain rate of 10^{-6} s^{-1}. The stress corrosion cracking susceptibility was evaluated by I_σ, I_δ and I_t, which were defined as the relative loss of tensile strength, elongation and time, respectively, to failure in air and in an aerated 3.5% NaCl solution with SSRT, as shown in Eqs. (1)−(3) [19].

$$I_\sigma = \frac{(\sigma_a - \sigma_c)}{\sigma_a} \times 100\% \quad (1)$$

$$I_\delta = \frac{(\delta_a - \delta_c)}{\delta_a} \times 100\% \quad (2)$$

$$I_t = \frac{(t_a - t_c)}{t_a} \times 100\% \quad (3)$$

where σ_a and σ_c are the tensile strength in air and in corrosion solution, respectively; δ_a and δ_c are the elongation in air and corrosion solution, respectively; t_a and t_c are the time to failure in air and corrosion solution, respectively. The larger relative loss reveals the higher stress corrosion cracking susceptibility.

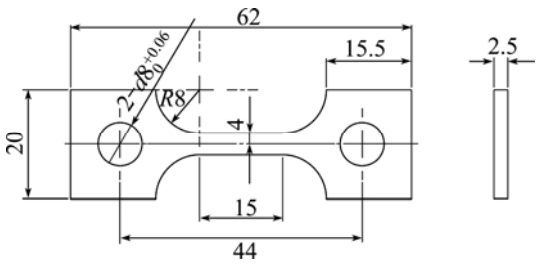

Fig. 1 Slow strain rate tensile sample (unit: mm)

Microstructural characterization was conducted by scanning electron microscopy (SEM) and energy dispersive X-ray spectrometry (EDS). The area fraction (f_A) of second phases was quantitatively measured over a number of SEM micrographs using an image analysis software. The micrographs and macrographs of fracture surfaces after SSRT were observed by SEM and stereo microscopy, respectively.

3 Results

3.1 Microstructures of 7050 alloys with different Si contents after T7651 treatment

Figure 2 shows the SEM images of longitudinal section parallel to the extruded direction of 7050-T7651 plates with different Si contents. The black and bright white particles are insoluble second phases above 1 μm in the three 7050-T7651 aluminum alloys. With the increase of Si content, the content and size are both increased obviously for the black particles, while they are reduced for the bright white particles. It can be identified that the black particles are Mg_2Si and the bright white particles consist of Al_2CuMg, Al_7Cu_2Fe and $Mg(Al,Cu,Zn)_2$ phases by EDS, as shown in Fig. 3. The types and chemical compositions of black and bright white particles are the same in the three alloys. The effects of Si content on the area fractions of black Mg_2Si and all of bright white phases are quantitatively estimated, as shown in Fig. 4. It can be seen that the area fraction of Mg_2Si increases from 0.16% to 0.32%, but the area fraction of bright white phases decreases drastically from 2.42% to 1.37% with increasing Si content from 0.094% to 0.134%. When the Si content further increases to 0.261%, the area fraction of Mg_2Si increases to 1.48%, while the area fraction of bright white phases decreases to 0.78%.

3.2 Electrical conductivity of three 7050 aluminum alloys

The influence of Si contents on electrical conductivity of 7050-T7651 aluminum alloys is shown in Fig. 5. The electrical conductivity increases from 36.5%

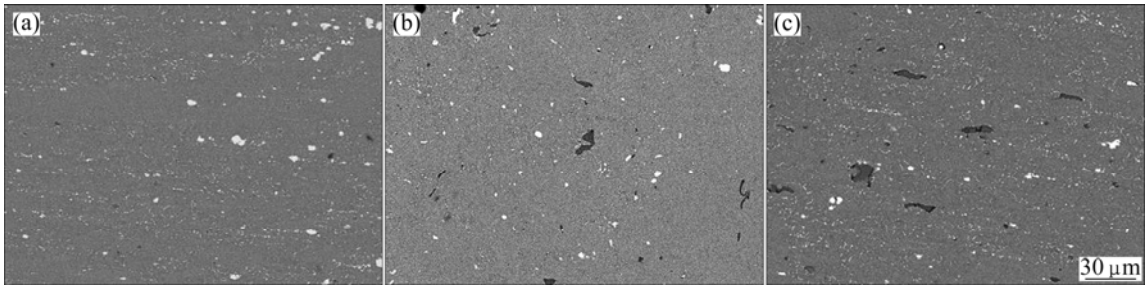

Fig. 2 SEM images of 7050-T7651 aluminum alloys with different Si contents: (a) Alloy 1; (b) Alloy 2; (c) Alloy 3

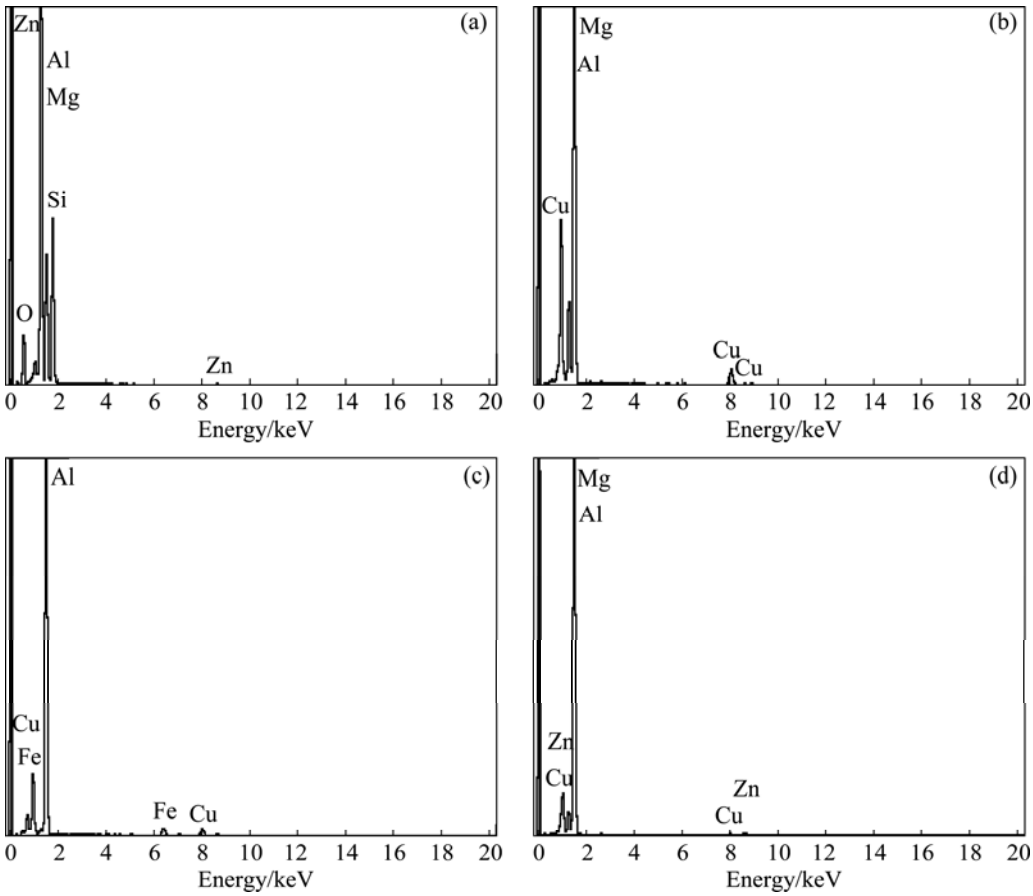

Fig. 3 EDS analysis of different second phase particles in 7050-T7651 aluminum alloys: (a) Mg_2Si; (b) Al_2CuMg; (c) Al_7Cu_2Fe; (d) $Mg(Al,Cu,Zn)_2$

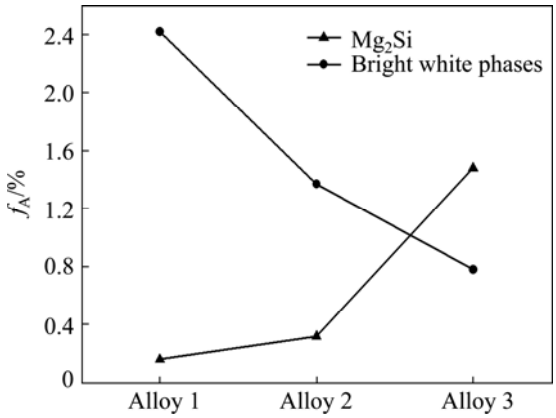

Fig. 4 Effects of Si content on area fraction of second phase particles in three 7050-T7651 aluminum alloys

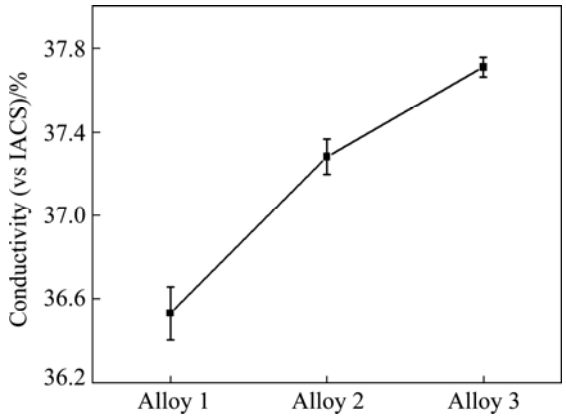

Fig. 5 Effects of Si content on electrical conductivity of 7050-T7651 aluminum alloy

to 37.3% (vs IACS) with Si content increasing from 0.094% to 0.134%. When the Si content further increases to 0.261%, the electrical conductivity increases to a higher level of 37.7% (vs IACS). The electrical conductivity is popularly used as one of the standards to evaluate the stress corrosion cracking resistance in industry [20]. A better stress corrosion cracking resistance is usually in company with higher electrical conductivity. Therefore, it can be inferred that the stress corrosion cracking resistance is improved with increasing Si content from 0.094% to 0.261% for 7050-T7651 aluminum alloys.

3.3 Stress corrosion

The tensile strength (σ_b), elongation (δ) and time to failure (t) were measured for the three 7050-T7651 aluminum alloys with SSRT in air and in 3.5% NaCl solution, respectively, and the relative losses of the three parameters were calculated by Eqs. (1)−(3), as listed in Table 1. When the alloys were tested in air, the tensile strength and time to failure decrease a little with increasing Si content from 0.094% to 0.134%, while the elongation has a small amount of improvement. With further increasing Si content to 0.261%, the tensile strength dramatically decreases to 478 MPa and the elongation and time to failure decrease as well. When the test was conducted in the 3.5% NaCl solution, the tensile strength, elongation and time to failure of three 7050-T7651 aluminum alloys all decrease compared with those in air, which indicates that the 7050-T7651 aluminum alloy has high stress corrosion cracking susceptibility.

The stress corrosion cracking susceptibility of three 7050-T7651 aluminum alloys with different Si contents were evaluated by the relative losses of tensile strength I_σ, elongation I_δ and time to failure I_t. I_σ increases a little, but I_δ and I_t all reduce with increasing the Si content from 0.094% to 0.134%. When the Si content increases to 0.261%, I_σ, I_δ and I_t all reduce to the least. As a result, the stress corrosion cracking susceptibility drops with increasing Si content from 0.094% to 0.261% based on the relative losses of tensile strength, elongation and time to failure with SSRT, which is in accordance with the results of electrical conductivity.

Figure 6 shows the SEM images of fracture surface of 7050-T7651 aluminum alloys with different Si contents by SSRT both in air and in 3.5% NaCl solution. In air, the fracture surfaces exhibit a dominant ductile transgranular fracture with small ductile dimples and a few of large dimples generated by decohesion between the matrix and coarse intermetallic particles for the three 7050-T7651 aluminum alloys, as shown in Figs. 6(a)−(c). However, the size and number of large dimples increase obviously in the case of 0.261% Si, which is corresponding with the increase of size and number of Mg_2Si. It is the main reason for decreasing the tensile strength and elongation of 7050-T7651 aluminum alloys with 0.261% Si by SSRT in air.

After being tested in 3.5% NaCl solution, the corrosion of fracture surfaces is alleviated by increasing Si content from 0.094% to 0.261%, as shown in Figs. 6(d)−(f). The fracture surface with 0.094% Si has the largest amount of corrosion products with a shape of globularity, while the amount of corrosion products is the least and some small ductile dimples can be clearly found on the fracture surface with 0.261% Si. It can also be seen that intergranular and secondary cracks occur in the three alloys, which is the characterization of brittle fracture. Figure 7 shows that the fracture surface has an angle of 45° to the axis of the tensile specimen with 0.094% Si, which is similar to the brittle fracture. With increasing Si content, the fracture surface tends to be perpendicular to the axis, denoting the improved ductility. According to the fracture characteristic, it can also be illustrated that the stress corrosion cracking susceptibility reduces with increasing Si content from 0.094% to 0.261% for 7050-T7651 aluminum alloys.

4 Discussion

In the microstructures of 7050-T7651 aluminum alloys, coarse Mg_2Si, Al_2CuMg, Al_7Cu_2Fe and $Mg(Al,Cu,Zn)_2$ are undissolved during homogenization and solution treatments, but distribute along the direction of extrusion. With increasing Si content, the content of Mg_2Si increases by depleting more Mg atoms, causing that the contents of the other Mg-rich phases decrease, including Al_2CuMg and $Mg(Al,Cu,Zn)_2$. Coarse Mg_2Si particle is easy to crack or separate from the matrix to form a void due to stress concentration under a low

Table 1 Tensile properties and stress corrosion cracking susceptibility of three 7050-T7651 aluminum alloys by SSRT

Sample No.	In air			In 3.5% NaCl solution			Relative loss		
	σ_b/MPa	δ/%	t/h	σ_b/MPa	δ/%	t/h	I_σ/%	I_δ/%	I_t/%
1	530	29.1	75.7	360	15.0	28.3	32.1	58.9	62.6
2	521	29.6	75.3	344	16.5	38.1	34.0	44.9	49.4
3	478	27.3	74.0	362	17.5	40.4	24.4	36.3	45.4

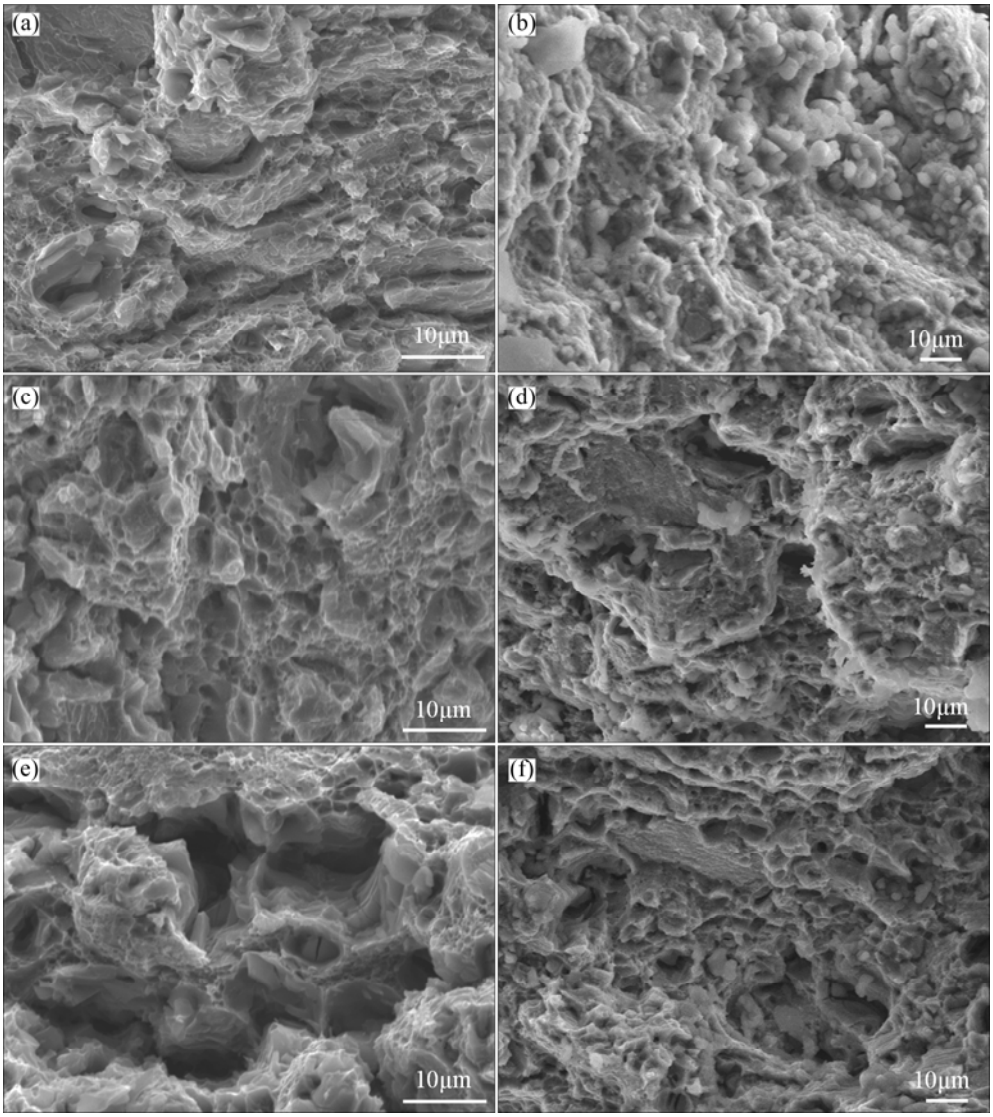

Fig. 6 Morphologies of SSRT fracture surfaces of 7050 aluminum alloys with different Si contents: (a) Alloy 1 in air; (b) Alloy 2 in air; (c) Alloy 3 in air; (d) Alloy 1 in 3.5% NaCl solution; (e) Alloy 2 in 3.5% NaCl solution; (f) Alloy 3 in 3.5% NaCl solution

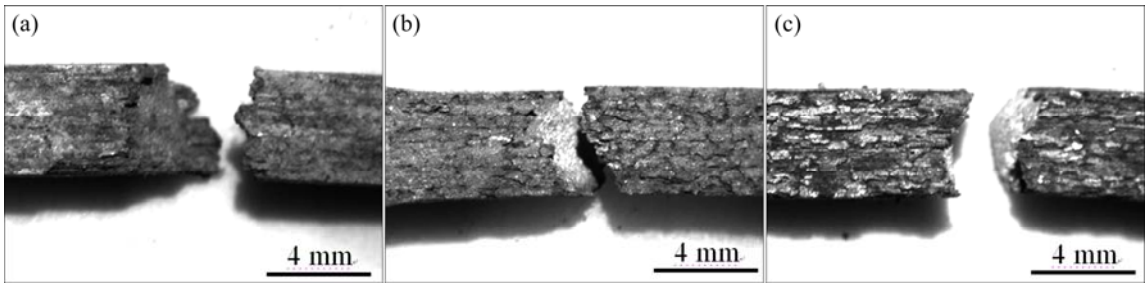

Fig. 7 Fracture macrographs of 7050-T7651 aluminum alloys by SSRT in 3.5% NaCl solution observed by stereo microscopy: (a) Alloy 1; (b) Alloy 2; (c) Alloy 3

stress, which results in the decrease of strength and ductility of aluminum alloys [21]. Thus, the largest size and number of coarse Mg_2Si particles give rise to the lowest tensile strength and elongation in 7050-T7651 aluminum alloy with 0.261% Si by SSRT in air, as listed in Table 1.

Electrical conductivity is strongly influenced by the lattice distortion of matrix originated from the point defects. The higher the concentration of the solute atoms is, the more serious the lattice distortion of matrix is and the more scattered the electron in matrix is. Therefore, the electrical conductivity drops with the increase of the

solute atom concentrations [22,23]. In addition, electrical conductivity is reduced with finer and more dispersive and uniform-distributed precipitates [22,24]. With the increase of Si content, the concentration of Mg atoms dissolved in Al matrix is reduced because of the increase of coarse Mg_2Si content, and the content of other Mg-rich phases decreases as well, which contributes to the improvement of electrical conductivity.

Stress corrosion cracking (SCC) is a type of brittle intergranular fracture usually, generated as a result of combined function of tensile stress and corrosion. Hydrogen embrittlement and anodic dissolution are the two dominant mechanisms for SCC [22]. Anodic dissolution depends on the difference of potential between the second phases and surrounding matrix, which not only provides an initial crack, but also promotes the production of hydrogen on the cathode, hence reducing the SCC resistance [8]. The potential of Al_7Cu_2Fe is lower than that of Al matrix, acting as a cathode to promote dissolution of the matrix, while the potential of Mg_2Si, Al_2CuMg, $Mg(Al,Cu,Zn)_2$ and $MgZn_2$ is higher than that of Al matrix, being anodes dissolved preferentially [17,25]. The area fraction of bright white particles (Al_2CuMg, Al_7Cu_2Fe and $Mg(Al,Cu,Zn)_2$) is decreased with increasing Si content (Table 1), but their sizes are similar in three 7050-T7651 aluminum alloys (Fig. 2), which implies that the spacing in bright white particles is enlarged. It has been reported that the second phases presenting discrete distributions are responsible for enhancing the SCC resistance [12,20,26]. Although the content of Mg_2Si is increased with the Si content, it becomes coarser and distributes much more discrete, which has a little impact on increasing the stress corrosion cracking susceptibility. However, the decreasing content of bright white particles and the enlargement in the spacing between them reduce the stress corrosion cracking susceptibility evidently.

5 Conclusions

1) With Si content increasing from 0.094% to 0.261%, the area fraction of Mg_2Si increases from 0.16% to 1.48% and the size becomes coarser, while the area fractions of the other coarse phases including Al_2CuMg, Al_7Cu_2Fe and $Mg(Al,Cu,Zn)_2$ decrease from 2.42% to 0.78% and the size is also reduced in 7050-T7651 aluminum alloys.

2) Electrical conductivity increases with Si content increasing from 0.094% to 0.261%, which is attributed to the reducing of the concentration of Mg atoms dissolved in Al matrix and the decreasing content of other Mg-rich phases.

3) The increase of size and content of coarse Mg_2Si with Si content increasing from 0.094% to 0.261% reduce the tensile strength and elongation by SSRT in air for 7050-T7651 aluminum alloys. However, the stress corrosion cracking susceptibility is reduced by increasing Si content due to the decreasing content of the other coarse phases and the enlargement in the spacing between them.

References

[1] HEINZ A, HASZLER A, KEIDEL C, MOLDENHAUER S, BENEDICTUS R, MILLER W S. Recent development in aluminium alloys for aerospace applications [J]. Materials Science and Engineering A, 2000, 280(1): 102−107.

[2] JAMES T S, JOHN L, WARREN H H Jr. Aluminum alloys for aero-structures [J]. Advanced Materials and Process, 1997, 152(4): 17−20.

[3] DIXIT M, MISHRA R S, SANKARAN K K. Structure–property correlations in Al 7050 and Al 7055 high-strength aluminum alloys [J]. Materials Science and Engineering A, 2008, 478(1−2): 163−172.

[4] STARINK M J, LI X M. A model for electrical conductivity of peak-aged and overaged Al−Zn−Mg−Cu alloys [J]. Metallurgical and Materials Transactions A, 2003, 34(4): 899−911.

[5] ADLER P N, DEIASI R, GESCHWIND G. Influence of microstructure on the mechanical properties and stress corrosion susceptibility of 7075 aluminum alloy [J]. Metallurgical Transactions, 1972, 12(3): 3191−3200.

[6] PARK J K, ARDELL A J. Effect of retrogression and reaging treatments on the microstructure of Al-7075-T651 [J]. Metallurgical and Materials Transactions A, 1984, 15 (8): 1531−1543.

[7] CHEN Song-yi, CHEN Kang-hua, PENG Guo-sheng, LIANG Xin, CHEN Xue-hai. Effect of quenching rate on microstructure and stress corrosion cracking of 7085 aluminum alloy [J]. Transactions of Nonferrous Metals Society of China, 2012, 22(1): 47−52.

[8] KNIGHT S P, BIRBILIS N, MUDDLE B C, TRUEMAN A R, LYNCH S P. Correlations between intergranular stress corrosion cracking, grain-boundary microchemistry, and grain-boundary electrochemistry for Al−Zn−Mg−Cu alloys [J]. Corrosion Science, 2010, 52(12): 4073−4080.

[9] OLIVEIRA A F Jr, de BARROS M C, CARDOSO K R, TRAVESSA D N. The effect of RRA on the strength and SCC resistance on AA7050 and AA7150 aluminum alloys [J]. Materials Science and Engineering A, 2004, 379(1−2): 321−326.

[10] MARLAUD T, DESCHAMPS A, BLEY F, LEFEBVRE W, BAROUX B. Evolution of precipitate microstructures during the retrogression and re-ageing heat treatment of an Al−Zn−Mg−Cu alloy [J]. Acta Materialia, 2010, 58(14): 4814−4826.

[11] LI J F, BIRBILIS N, LI C X, JIA Z Q, CAI B, ZHRNG Z Q. Influence of retrogression temperature and time on the mechanical properties and exfoliation corrosion behavior of aluminium alloy AA7150 [J]. Materials Characterization, 2009, 60 (11): 1334−1341.

[12] PENG Guo-sheng, CHEN Kang-hua, CHEN Song-yi, FANG Hua-chan. Influence of repetitious-RRA treatment on the strength and SCC resistance of Al−Zn−Mg−Cu alloy [J]. Materials Science and Engineering A, 2011, 528(12): 4014−4018.

[13] HUANG Lan-ping, CHEN Kang-hua, LI Song. Influence of grain-boundary pre-precipitation and corrosion characteristics of inter-granular phases on corrosion behaviors of an Al−Zn−Mg−Cu alloy [J]. Materials Science and Engineering B, 2012, 177(11): 862−868.

[14] ANDREATTA F, TERRYN H, de Wit J H W. Effect of solution heat treatment on galvanic coupling between intermetallics and matrix in AA7075-T6 [J]. Corrosion Science, 2003, 45(8): 1733−1746.

[15] ZHANG Ping, LI Qi, ZHAO Jun-jun, ZENG Qing-qiang. Analysis of secondary phases and measurement of volta potential of 7A52 aluminum alloy [J]. The Chinese Journal of Nonferrous Metals, 2011, 21(6): 1252−1257. (in Chinese)
[16] VENUGOPAL A, PANDA R, MANWATKAR S, SREEKUMAR K, RAMA KRISHNA L, SUNDARARAJAN G. Effect of micro arc oxidation treatment on localized corrosion behaviour of AA7075 aluminum alloy in 3.5% NaCl solution [J]. Transactions of Nonferrous Metals Society of China, 2012, 22(3): 700−710.
[17] WLOKA J, BURKLIN G, VIRTANEN S. Influence of second phase particles on initial electrochemical properties of AA7010-T76 [J]. Electrochimica Acta, 2007, 53(4): 2055−2059.
[18] LU Hai-qing, ZHANG Si-ping. Study on process of 7075-T7651 aluminum alloy prestretched plate [J]. Aluminum Fabrication, 2004, 4: 48−51. (in Chinese)
[19] CHI Lin. Fundamental research of SCC behavior and detection technology of pipeline steel [D]. Beijing: Beijing University of Chemical Technology, 2004. (in Chinese)
[20] LI Hai, ZHENG Zi-qiao, WANG Zhi-xiu. Influence of heat treatment regime on microstructures and fracture characteristics of 7055 Al alloy containing Ag [J]. Rare Metal Materials and Engineering, 2005, 34(4): 612−616. (in Chinese)
[21] VRATNICA M, PLUVINAGE G, JODIN P, CVIJOVIC Z, RAKIN M, BURZIC Z. Influence of notch radius and microstructure on the fracture behavior of Al−Zn−Mg−Cu alloys of different purity [J]. Materials Design, 2010, 31(4): 1790−1798.
[22] CHEN Song-yi, CHEN Kang-hua, PENG Guo-sheng, FANG Hua-chan. Effects of solution temperature on microstructure and stress corrosion of Al−Zn−Mg−Cu aluminum alloy [J]. Materials Science and Engineering of Powder Metallurgy, 2010, 15(5): 456−462. (in Chinese)
[23] RANGANATHA R, ANIL KUMAR V, NANDI V S, BHAT R R, MURALIDHARA B K. Multi-stage heat treatment of aluminum alloy AA7049 [J]. Transactions of Nonferrous Metals Society of China, 2013, 23(6): 1570−1575.
[24] ZANG Jin-xin, ZHANG Kun, DAI Sheng-long. Precipitation behavior and properties of a new high strength Al−Zn−Mg−Cu alloy [J]. Transactions of Nonferrous Metals Society of China, 2012, 22(11): 2638−2644.
[25] LI J C, LIAO H L, JEHNG W D. Effect of heat treatments on the tensile strength and SCC- resistance of AA7050 in an alkaline saline solution [J]. Corros Science, 2006, 48(10): 3139−3156.
[26] PENG Guo-sheng, CHEN Kang-hua, CHEN Song-yi, FANG Hua-chan. Influence of dual retrogression and re-aging temper on microstructure, strength and exfoliation corrosion behavior of Al−Zn−Mg−Cu alloy [J]. Transactions of Nonferrous Metals Society of China, 2012, 22(4): 803−809.

Si 含量对 7050 铝合金显微组织和抗应力腐蚀开裂的影响

佘 欢[1], 储 威[1], 疏 达[1], 王 俊[1,2], 孙宝德[1,2]

1. 上海交通大学 上海市先进高温材料及其精密成形重点实验室，上海 200240；
2. 上海交通大学 金属基复合材料国家重点实验室，上海 200240

摘 要：分别研究 Si 含量为 0.094%、0.134%和 0.261%的 3 种 T7651 态 7050 铝合金的组织和应力腐蚀开裂敏感性。结果表明：随着 Si 含量从 0.094%增加到 0.261%，Mg_2Si 相的面积分数从 0.16%增加到 1.48%，并且尺寸粗化；而其它粗大相(包括 Al_2CuMg、$Mg(Al,Cu,Zn)_2$ 和 Al_7Cu_2Fe)的面积分数从 2.42%减小到 0.78%。合金的电导率随 Si 含量的增加而增加。合金在空气中进行慢应变速率拉伸时，抗拉强度和伸长率随 Si 含量的增加而降低；而在 3.5%NaCl 溶液中进行慢应变速率拉伸时，随 Si 含量增加，合金应力腐蚀开裂敏感性降低。

关键词：7050 铝合金；Si 含量；显微组织；抗应力腐蚀开裂

(Edited by Chao WANG)